Kovove Mater. 61 2023 1–11
DOI: 10.31577/km.2023.1.1

Numerical simulation of thermal conductivity of graphite flake/Cu composites with interfacial characteristics

Jingyang Nan[1]*, Xinbo He[1,2], Zhang Tao[1,2], Xuanhui Qu[1,3], Haiqing Yin[3]

[1] *Institute for Advanced Materials and Technology, University of Science and Technology Beijing, Beijing 100083, P. R. China*
[2] *New Materials Research Institute Guangzhou, University of Science and Technology Beijing, Guangzhou 510330, P. R. China*
[3] *Beijing Advanced Innovation Center for Materials Genome Engineering, Beijing 100083, P. R. China*

Received 25 October 2021, received in revised form 16 November 2021, accepted 11 November 2022

Abstract

Graphite flake (GF)/Cu composites have received much attention as a promising thermal management material. This work provides a homogenization method to examine the effect of interfacial characteristics on the thermal conductivity of GFs/Cu composite. The finite element homogenization method is used to establish models of representative volume elements of material microstructure and interfacial layers, respectively, considering the distribution morphology and thermophysical properties of interface compositions. The interfacial layers are considered equivalent heat conduction materials, including interface compositions, pores, and Kapitza thermal resistances between compositions. The results of the thermal conductivity obtained by the approach were compared with the experimental results in the literature, and it shows good agreement. The results have indicated that the thermal conductivity of GFs/Cu composites is strongly affected by graphite sizes, graphite volume contents, interface contents, pore shapes, the relative density of interfacial layers, and whether the interface component is continuous has a significant influence.

K e y w o r d s: effective thermal conductivity, Kapitza thermal resistance, finite element method, graphite flake/Cu composite, microstructure, relative density

Nomenclature

TC	thermal conductivity
λ	thermal conductivity
Cu	copper
GFs	graphite flakes
C_{p}	specific heat capacity
ρ	density
T	temperature
q	heat flux
h	convective heat transfer coefficient
C_{m}	specific heat capacity of the matrix
v	the Debye phonon velocity
L	longitudinal dimension of model
ρ_{c}	relative density of the composite
ρ_{in}	relative density of the interfacial layer
d	length of the graphite flake
t_i	thickness of components
$t_{\mathrm{in},i}$	thickness of interfacial layer with TiC/Cr_3C_2
V_{GF}	the volume fraction of GFs
$R_{\mathrm{k},ij}$	Kapitza thermal resistance between two components
$K_{\mathrm{r},ij}$	TC of the thin layer represents R_{k} between two components
$K_{\mathrm{in},i}$	equivalent TC of the interfacial layer with TiC/ Cr_3C_2
$K_{\mathrm{c},i}$	equivalent TC of composites
$K_{\mathrm{in,p}}$	equivalent TC of the interfacial layer with a pore
$R_{\mathrm{in},i}$	the interfacial thermal resistance with TiC/Cr_3C_2
Model 1a	model of the interfacial layers with TiC
Model 1b	model of the interfacial layers with Cr_3C_2
Model 2	model of GFs/Cu composite with an interfacial layer

*Corresponding author: e-mail address: 695946690@qq.com

Subscript			
1	component 1 (amorphous carbon)	m	matrix
2	component 2 (TiC)	re	reinforcement component phase
3	component 3 (Cr_3C_2)	in	interfacial layer
4	graphite flake	Y	longitudinal direction
5	copper	X	transversal direction
i, j	each component	con	continuous
		dis	discontinuous

1. Introduction

Heat dissipation capability in modern micro-electronic devices has become extremely important with the power electronic devices toward miniaturization and integration. It is vitally important to develop thermal management materials with high thermal conductivity (TC) and tailored coefficient of thermal expansion (CTE) values to minimize thermal stresses [1, 2]. Metal matrix composites combining the high TC of metal and low CTE of the reinforcement can be suitable candidates for electronic packaging materials [3]. Recently, GFs-reinforced copper matrix composites have gained much attention due to their excellent thermal properties, low density, and good machinability.

Determining the equivalent TC is essential for the design and preparation of composites and performance research [4]. Maxwell assumed a perfect thermal connection between the matrix and filler to calculate the TC. Then, the Hasselman-Johnson model is widely used to describe the TC of a composite by introducing interfacial thermal resistance [5]. Several theoretical models have been established to predict the thermal conduction of particle-reinforced composites [6–8]. Vignesh P. used Representative Volume Element (RVE) technique to evaluate the material properties of Al-SiC composite [9]. Vieira C. proposes a three-dimensional micromechanical model for evaluating the effective TC of multiphase composites with periodic microstructure [10]. Saoudi T. used the numerical homogenization technique to evaluate the representative volume element and to compute the effective thermal properties of fiber-reinforced composites [11]. Zahid M. presented a micro-structurally informed two-scale unit cell analysis for the prediction of thermal conductivities of carbon/carbon composites [12]. Duschlbauer D. predicted the TC of fiber composites based on FEM, in which the effect of thermal barrier resistance is taken into account [13]. To describe the TC of particulate-filled composites with inhomogeneous interfacial thermal conductances and particle shape, the Finite Element Method (FEM) is used to describe the thermal properties of heterogeneous materials system [6, 14, 15].

However, the effect of the interface structure on GFs/Cu composites has yet to be reported. This work provides theoretical guidance to evaluate the effects of different interfacial layers. The extended Acoustic Mismatch Model (AMM) is developed to calculate the Kapitza thermal resistances, and model of representative volume elements (RVE) established by Abaqus is applied to calculate the TC of composites, and quantitatively analyze the influence of the interfacial layers on the TC of the composite and research which factors will strongly or weakly affect material properties. An example of composites with different graphite volume contents of TiC and Cr_3C_2 interfacial layers, together with the experimental results from the references, is provided to verify the rationality of the method.

2. Method

2.1. Finite element modeling

Based on the homogenization theory, this work selects the microscopic units in the composite that can accurately reflect its composition characteristics to build the model, which is the representative volume element (RVE). As shown in Fig. 1, these two pictures are cross-sectional views of the interfacial layer and GFs/Cu composite taken by SEM [16]. In Fig. 1a, there are coated metal carbides and amorphous carbon at the interface of Cu and GFs.

Model 1a, Model 1b, and Model 2 are established to describe the microstructure of the interfacial layers and composite. The size ratio of the model to the real object is 1 : 1, as shown in Figs. 2 and 3. According to Delesse's law in stereology, the percentage of two-dimensional area measured on a random interface is equivalent to the corresponding volume percentage in three-dimensional space [17].

In Model 1a and Model 1b, the four partitions from top to bottom are GFs, amorphous carbon, TiC/Cr_3C_2, and Cu. According to experimental measurement [18], in Fig. 2a: $t_1 = 65$ nm, $t_2 = 600$ nm; in Fig. 2b: $t_1 = 8$ nm, $t_3 = 700$ nm.

Model 1a and Model 1b are used to calculate the equivalent TC of the interfacial layer K_{in}, and then in Model 2, the interfacial layer is regarded as a new hypothetical substance to calculate the TC of the composite K_{c}. The other thermophysical parameters of the interfacial layer are weighted by the volume fraction. Many studies have reported that the TC of composites in the Z direction is lower than 80 W m^{-1} K^{-1}, which suffers from the low TC in the graphite c-axis, and no further discussion is necessary. In the following

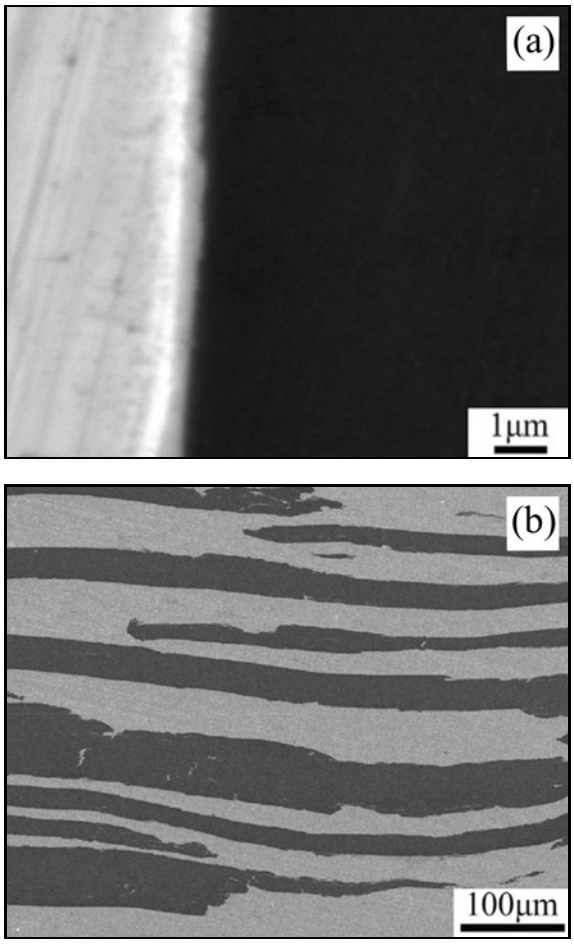

Fig. 1. Typical SEM micrograph of (a) GFs/Cu composite with TiC coating and (b) the interface for GFs/Cu-Ti.

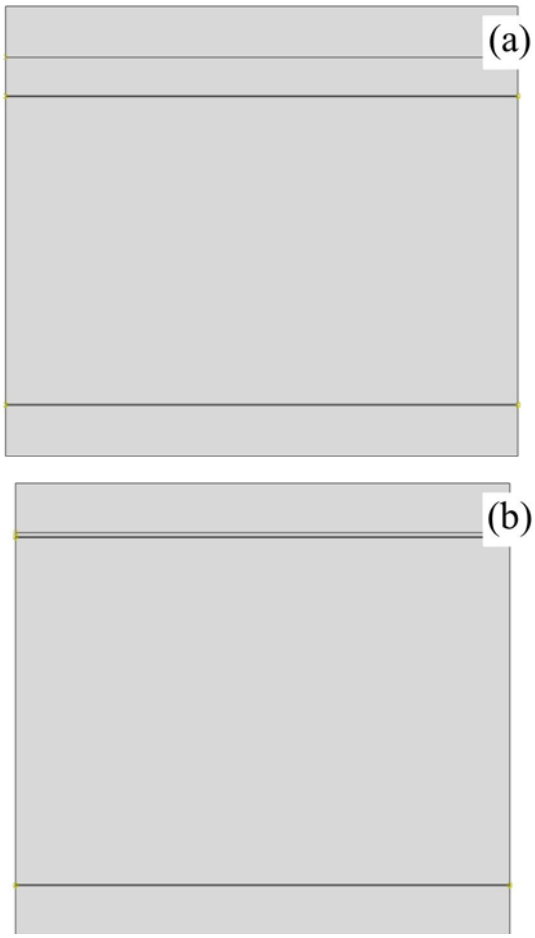

Fig. 2. Models used for predicting the TC of the interfacial layers of (a) TiC-coated GFs/Cu composite and (b) Cr_3C_2 coated GFs/Cu composite.

discussion, we will focus on the TC in the X-Y plane.

2.2. Material parameters and boundary conditions

According to the thermal conductivity theory of composite [19, 20], the temperature at the interface of two materials in perfect contact is not continuous because of the Kapitza thermal resistance (R_k) [21], which can be expressed as:

$$R_\mathrm{k} = \frac{\Delta T}{q}\ (^\circ\mathrm{C}). \tag{1}$$

The R_k has a significant impact on the TC of the composite [22, 23]. The R_k of each interface can be calculated by Acoustic Mismatch Model (AMM) [24], which can be expressed as:

$$R_\mathrm{k} = \frac{2\left(\rho_\mathrm{m} v_\mathrm{m} + \rho_\mathrm{re} v_\mathrm{re}\right)}{c_\mathrm{m}\rho_\mathrm{re} v_\mathrm{re}\rho_\mathrm{m}^2 v_\mathrm{m}^2}\left(\frac{v_\mathrm{re}}{v_\mathrm{m}}\right)^2. \tag{2}$$

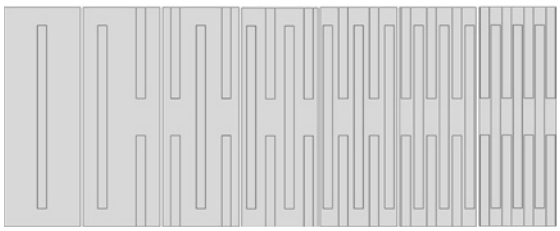

Fig. 3. Models used for Ti-coated GFs/Cu composite with 10–70 % volume fractions.

The average phonon velocity of graphite is:

$$\frac{2}{v^2} = \frac{2}{v_\mathrm{l}^2} + \frac{2}{v_\mathrm{t}^2}. \tag{3}$$

Amorphous carbon is produced by fracturing sp^2 C-C bonds in graphite and has a higher proportion of sp^2C-C bonds. Therefore, amorphous carbon can be regarded as a short-range ordered graphite crystal,

Table 1. Material parameters for model predictions

Materials	Density ($kg\,m^{-3}$)	Thermal conductivity ($W\,m^{-1}\,K^{-1}$)	Specific heat ($J\,kg^{-1}\,K^{-1}$)	Phonon velocity ($m\,s^{-1}$)
Cu	8960	400	385	2881
TiC	4930	36.4	562	6777
Cr_3C_2	6680	19	456	5493
Graphite	2260	1000	710	14800

so the R_k between graphite and amorphous carbon can be ignored. Table 1 shows the material parameters used in FEM heat transfer analysis and AMM calculation [25–27].

In Model 1a and Model 1b, the R_k of each interface is represented by an assumed thin layer. If the thickness of the thin layer is 2 nm, the TC of the thin layer is expressed as:

$$K_r = \frac{2 \times 10^{-9}}{R_k}, \tag{4}$$

where after calculation $K_{r,12} = 0.99\,W\,m^{-1}\,K^{-1}$, $K_{r,25} = 0.442\,W\,m^{-1}\,K^{-1}$, $K_{r,13} = 0.574\,W\,m^{-1}\,K^{-1}$, and $K_{r,35} = 0.662\,W\,m^{-1}\,K^{-1}$.

There are mainly steady-state and dynamic methods for simulating and calculating the TC of composites. In steady-state heat conduction analysis, temperature and heat flux meet the following equations:

$$\frac{\partial}{\partial x}\left(\lambda\frac{\partial T}{\partial x}\right) + \frac{\partial}{\partial y}\left(\lambda\frac{\partial T}{\partial y}\right) = 0, \tag{5}$$

$$q_x = -\lambda\frac{\partial T}{\partial x};\ q_y = -\lambda\frac{\partial T}{\partial y}. \tag{6}$$

Assuming the heat transfer direction is the y direction, the vertical direction is the x direction.

The upper boundary of the model is loaded with heat flux density, and the lower boundary is the heat transfer boundary, which is expressed as:

$$\lambda\frac{\partial T}{\partial x} + \lambda\frac{\partial T}{\partial y} = h\left(T_f - T_s\right), \tag{7}$$

where T_f and T_s are the ambient temperature and the bottom surface temperature.

The TC is calculated when the steady state (temperature difference $< \pm\ 0.1\,℃\,min^{-1}$) is reached. According to the standard ASTM: E1225-99 ASTM (1999), the following equation is used for calculation:

$$K = \frac{qL}{\Delta T}, \tag{8}$$

where T is the temperature difference between the upper and lower surfaces, obtained by averaging the surface temperatures. When calculating, $q = 500\,W\,m^{-2}$, $h = 1000\,W\,m^{-2}\,K^{-1}$, and the ambient temperature is 20 ℃. The other boundaries are insulated boundaries. As a test, three different heat flux densities were set, and three identical results were obtained, verifying the reliability of the model.

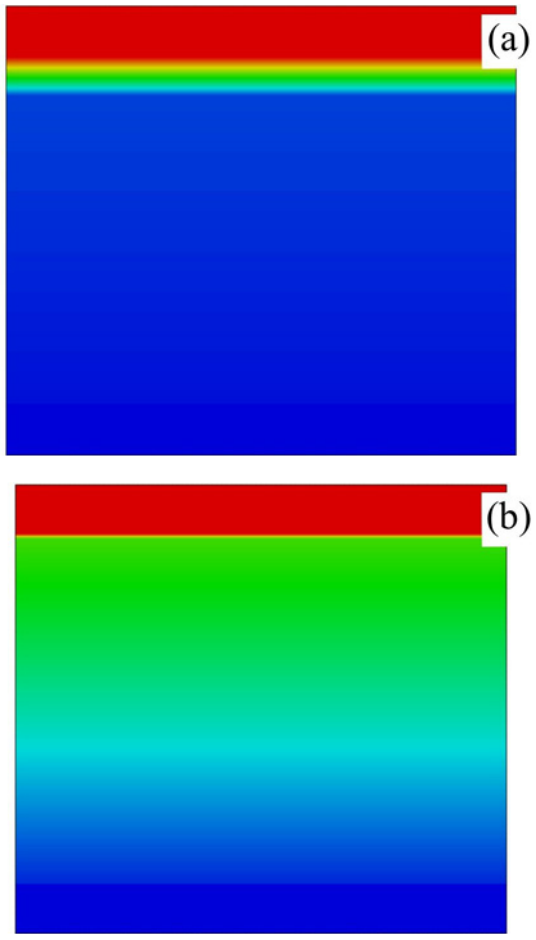

Fig. 4. The temperature field of TiC (a) and Cr3C2 (b) interfacial layers.

3. Results and discussion

3.1. Effect of graphite volume content and carbide interfacial layers

As shown in Fig. 4, it is the temperature field dis-

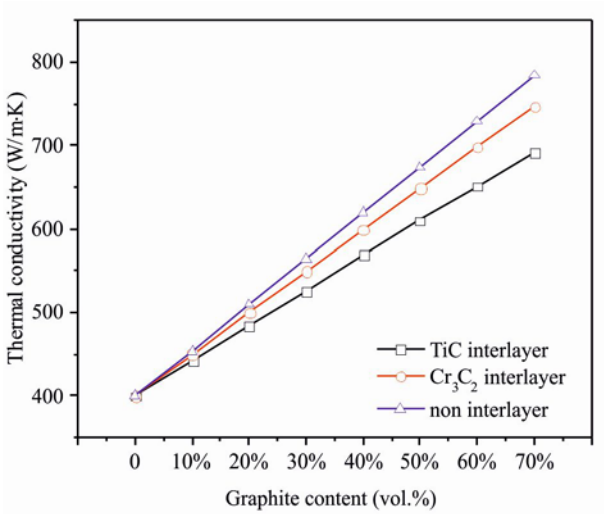

Fig. 5. The effect of graphite volume content on the TC of composites with different interfaces.

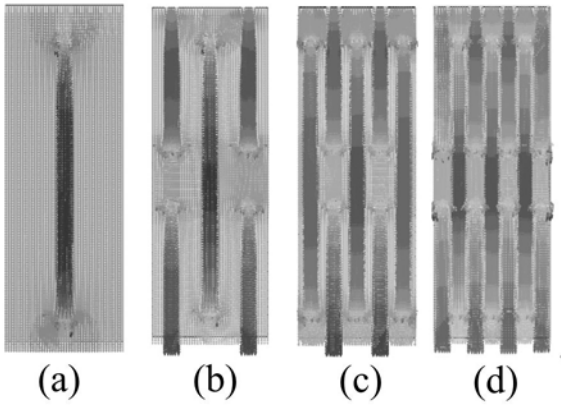

Fig. 6. Heat flux density field of the composite V_{GF}: (a) 10 %, (b) 30 %, (c) 50 %, and (d) 70 %.

tribution of the interfacial layers. The thickness of the interfacial layers $t_{in,2} = 675\,nm$ and $t_{in,3} = 708\,nm$ [28], the equivalent thermal resistance of the two interfacial layers is $R_{in,2} = 2.72 \times 10^{-7}\,m^2\,K\,W^{-1}$, $R_{in,3} = 6.99 \times 10^{-8}\,m^2\,K\,W^{-1}$. Model 1a and Model 1b are used for calculation, and the equivalent TC of the interfacial layers of the TiC-coated GFs/Cu composite is $K_{in,2} = 2.486\,W\,m^{-1}\,K^{-1}$. When Cr_3C_2 is coated, the value is $K_{in,3} = 10.13\,W\,m^{-1}\,K^{-1}$.

When there is a perfect interface between graphite and Cu, $R_{k,45} = 4.1 \times 10^{-9}\,m^2\,K\,W^{-1}$, if the thickness of the assumed thin layer representing R_k is 2 nm, $K_{in,45} = 0.4878\,W\,m^{-1}\,K^{-1}$. In practice, to improve the interface bonding, the interfacial layer has to be introduced. The TC of the composite with different interfacial conditions ($K_{c,2}$, $K_{c,3}$, $K_{c,non}$) and different graphite volume fractions is shown in Fig. 5.

It can be seen in Fig. 5 that as the volume fraction of graphite (V_{GF}) increases, the TC of the composites with three interface conditions increases, which is consistent with the conclusions of published experimental studies [28]. This is also consistent with the law obtained by X. Han et al. in experimental research [29]: as the volume fraction of the reinforcing phase increases, the TC of the composite increases. When V_{GF} increases from 0 to 70 %, $K_{c,2}$, $K_{c,3}$, and $K_{c,non}$ increase by 72.72, 86.75, and 95.86 %, respectively. The thermal resistance of the interfacial layer (R_{in}) is expressed as:

$$R_{in} = \frac{T_i}{K_{in,i}}. \tag{9}$$

It can be seen that $R_{in,2} > R_{in,3} > R_{in,non}$. The greater the TC of the interfacial layer, the smaller the R_{in}, the smaller the barrier effect of the interfacial layer on heat flow, and the larger the TC increases with the volume fraction, because the interfacial layer weakens the enhancement effect of the GFs on the TC.

In Fig. 6, the heat flows from the hot end to the cold end, and the heat flux density at the GFs is higher than the matrix part. Due to the minimum thermal resistance theory, heat preferentially selects the direction with smaller thermal resistance as the heat conduction channel. As V_{GF} increases, the high TC of the GFs itself increases the TC of the material. In addition, the heat flow in Fig. 6 is constant, and the increase of V_{GF} makes the difference in heat flow density between GFs and the matrix smaller, indicating that the heat conduction path between GFs increases, which in turn promotes the TC of the composite.

3.2. Effect of particle size and carbide interfacial layers

Substituting the $K_{in,2}$ and $K_{in,3}$ calculated in 3.1. section into the composite structure model with a graphite volume fraction of 30 %, and calculating the TC of the composite $K_{c,2,}$ and $K_{c,3}$ that changes with the size of GFs, gives results shown in Fig. 7.

From the rising trend of the two curves in Fig. 7, it can be seen that as the size of the GFs in the heat transfer direction (d) increases, $K_{c,2}$, and $K_{c,3}$ increase, but the increasing trend gradually decreases. When V_{GF} is constant, d increases, and the introduced interface decreases. Then the hindrance of the interface to heat conduction is reduced, and the TC of the composite is increased. Compared with experimental data, consistent results can be obtained [18]. Therefore, to increase the TC of the composite, the size of the reinforcing phase should be appropriately increased. Unlike the experimental results, the curve in Fig. 7 does not show a downward trend because the size effect has always existed, and the reduction of TC in the experiment is related to other process factors.

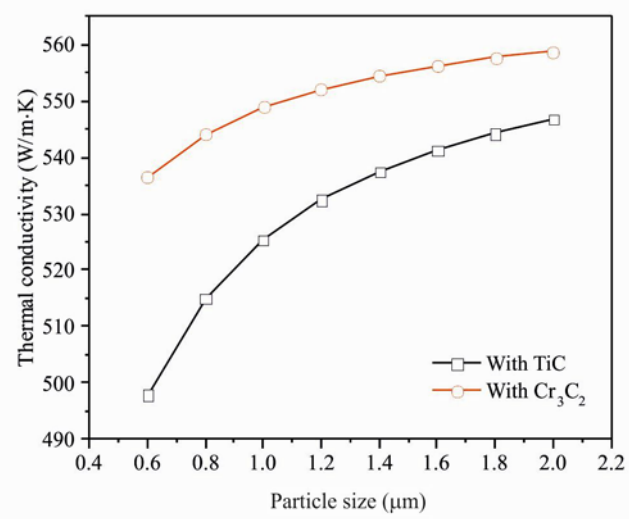

Fig. 7. Effect of GFs size on the TC of composite with different interfaces.

The growth rate of $K_{c,2}$ is greater than that of $K_{c,3}$. This is because $R_{in,2} > R_{in,3}$, the interfacial layer with considerable thermal resistance has a more significant blocking effect on heat flow. In summary, the smaller the thermal resistance of the interfacial layer between the reinforcing phase and the matrix, the more pronounced the effect of the size of the reinforcing phase on the TC of the composite.

3.3. Effect of the thickness of the interface compositions

To improve the interface bonding, the composite has to introduce interfacial layers. Assuming that the interfacial layer is a homogeneous heat transfer material, when the proportion of a component in the interfacial layer changes, the TC of this equivalent heat transfer composite $K_{in,2}$ also changes, as shown in Fig. 8. This section analyzes the influence of the thickness of TiC and amorphous carbon layer changes on $K_{in,2}$ and $K_{c,2}$. However, the increase in $K_{in,2}$ does not mean that the interfacial layer has a reduced hindrance to the heat flow in the composite because the thickness of the interfacial layer has also changed.

When analyzing the influence of TiC thickness, $t_1 = 75$ nm; when analyzing amorphous carbon, $t_2 = 600$ nm; $V_{GF} = 30$ %. From the downward trend of the curve in Fig. 9, it can be seen that when the thickness of the TiC layer and the amorphous carbon layer in the interface increases, $K_{c,2}$ decreases. Because the thickness of the interface phase increases, R_{in} increases, and the hindrance of the interface to the heat flow becomes more apparent. Part of the heat flow passes through the GFs, and another part of the heat flow is blocked by the interface and bypasses the GFs. This leads to a longer heat transfer path.

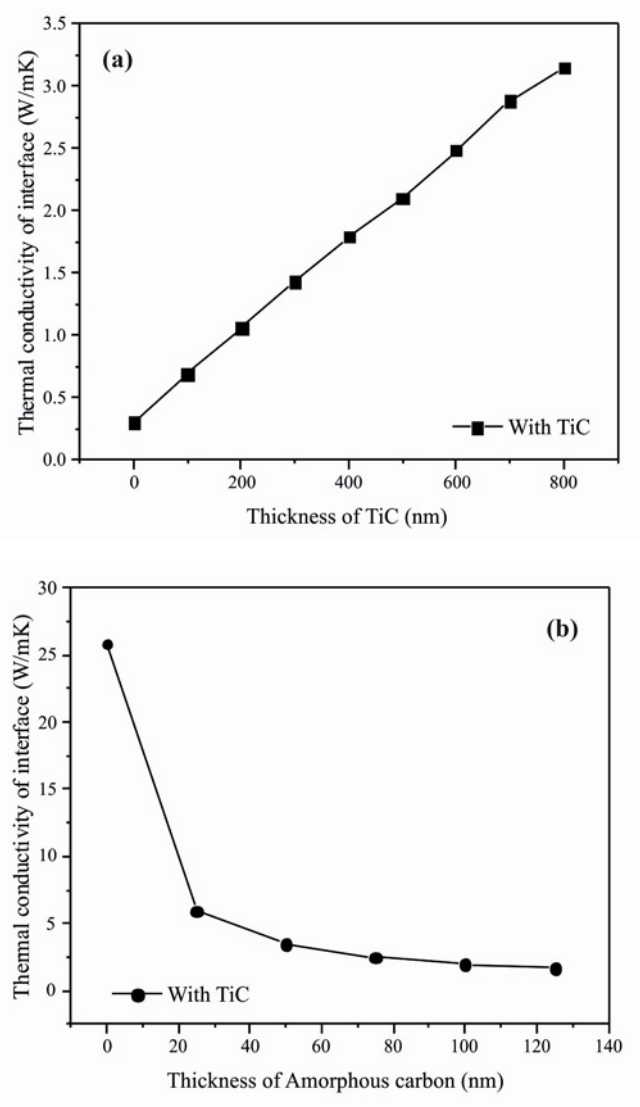

Fig. 8. Effect of the thickness of (a) TiC and (b) amorphous carbon on the TC of the interfacial layer.

TiC with a thickness of 600 nm and amorphous carbon with a thickness of 75 nm reduce $K_{c,2}$ by 5.63 and 46.69 $W\,m^{-1}\,K^{-1}$, respectively, indicating that amorphous carbon has a more significant impact on $K_{c,2}$, because the intrinsic TC of the amorphous carbon is smaller than that of TiC. The interface with a smaller thickness facilitates the formation of heat conduction channels inside the composite. However, in actual situations, if the interface thickness is too thin, it will cause defects such as cracks and voids in the interface, and it is difficult for graphite to be wrapped entirely, which seriously affects the heat transfer of the composite. Therefore, an interfacial layer of appropriate thickness should be designed, and the amorphous carbon content should be minimized.

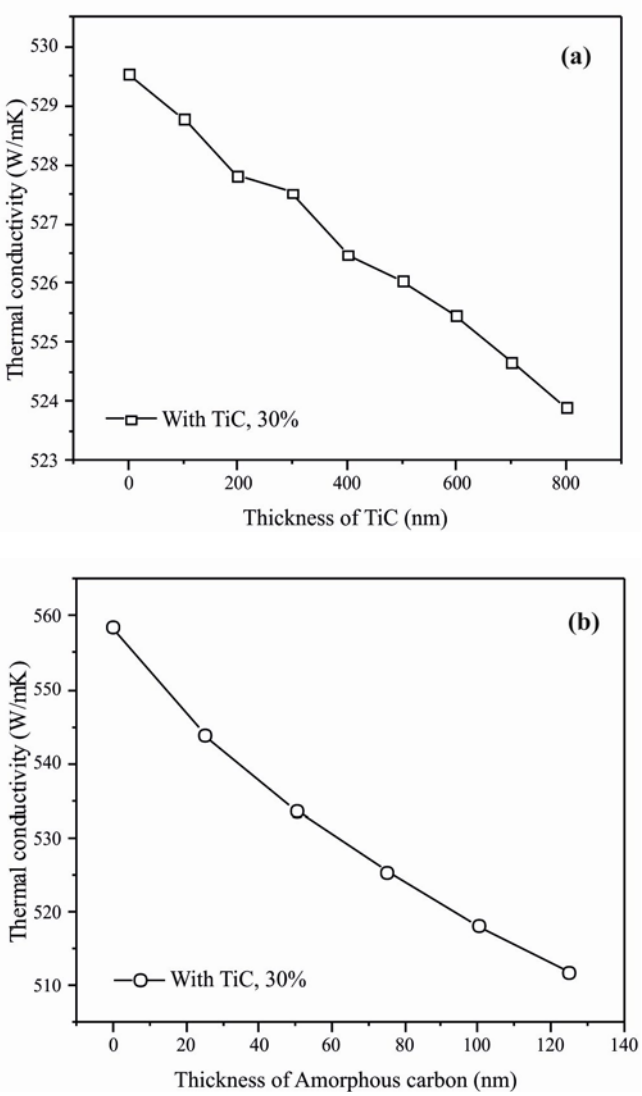

Fig. 9. Effect of the thickness of (a) TiC nad (b) amorphous carbon on the TC of the composite.

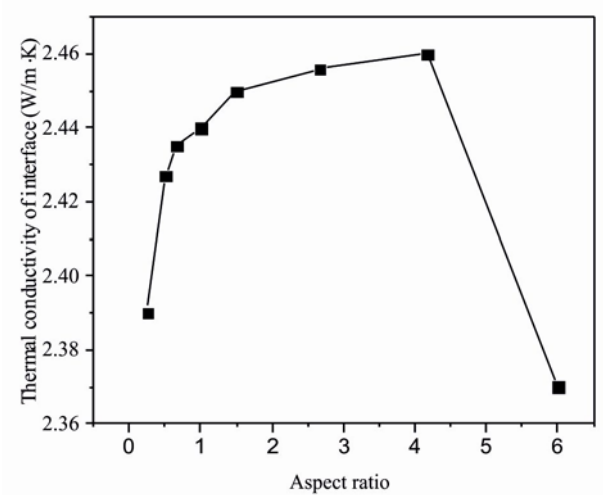

Fig. 10. Effect of the aspect ratio of pores on the TC of the interfacial layer.

3.4. *Effect of pores in the interfacial layer*

Air pores are a common defect, often appearing at the contact interface between the reinforcing phase and the metal matrix, and seriously affects the TC of the composite. Since the distribution, size, and shape of the pores are difficult to be quantitatively processed through experiments, this section uses simulation methods to study the effects of different pore shapes, pore sizes, and porosity on the TC of composites.

Let us assume that the position of the pore is at the interface between carbide and Cu. In the enclosed space, there is a compound heat exchange of natural convection, heat conduction, and radiation. The Rayleigh number in the judgment of convective heat transfer at the pores is extremely small, so convective heat transfer and radiation heat transfer are extremely small and can be ignored, so the heat transfer method at the pores is heat conduction [30]. At 20 ℃, the TC of air is 0.0257 $\mathrm{W\,m^{-1}\,K^{-1}}$, the density is 1.2 $\mathrm{kg\,m^{-3}}$, and the specific heat capacity is 1.005 $\mathrm{J\,kg^{-1}\,K^{-1}}$ [31]. The equivalent TC of the interfacial layer with pores ($K_{\mathrm{in,p}}$) is calculated, and then the value is substituted into the composite model to calculate $K_{\mathrm{c},2}$.

3.4.1. *Effect of the shape of pores*

Assuming that the pores are rectangular, the volume fraction of the pores in the interfacial layer is 10 %, and the interval of each pore distribution is 1000 nm. After heat transfer analysis, $K_{\mathrm{in,p}}$ changes with the pore aspect ratio, that is, the ratio of the longitudinal dimension (in the direction of heat flow/Y--direction) to the lateral dimension (perpendicular to the direction of heat flow/X-direction), as shown in Fig. 10.

In Fig. 10, when the aspect ratio is less than 6, the larger the aspect ratio, the greater the TC of the interfacial layer, indicating that the influence of the pore on $K_{\mathrm{in,p}}$ is more negligible. At the current porosity, when the aspect ratio is 6, the length of the pore has penetrated the TiC layer, and how the pore affects the thermal conductivity of the interfacial layer has changed. In detail, when the pore length does not exceed the thickness of the TiC layer, that is, when the interfacial layer is continuous, the pores only reduce the thermal conductivity of the interface between copper and TiC. When the pore length exceeds the thickness of the TiC layer, the pores simultaneously reduce the thermal conductivity of the copper-TiC interface and the amorphous carbon-TiC interface, so the thermal conductivity of the entire interfacial layer

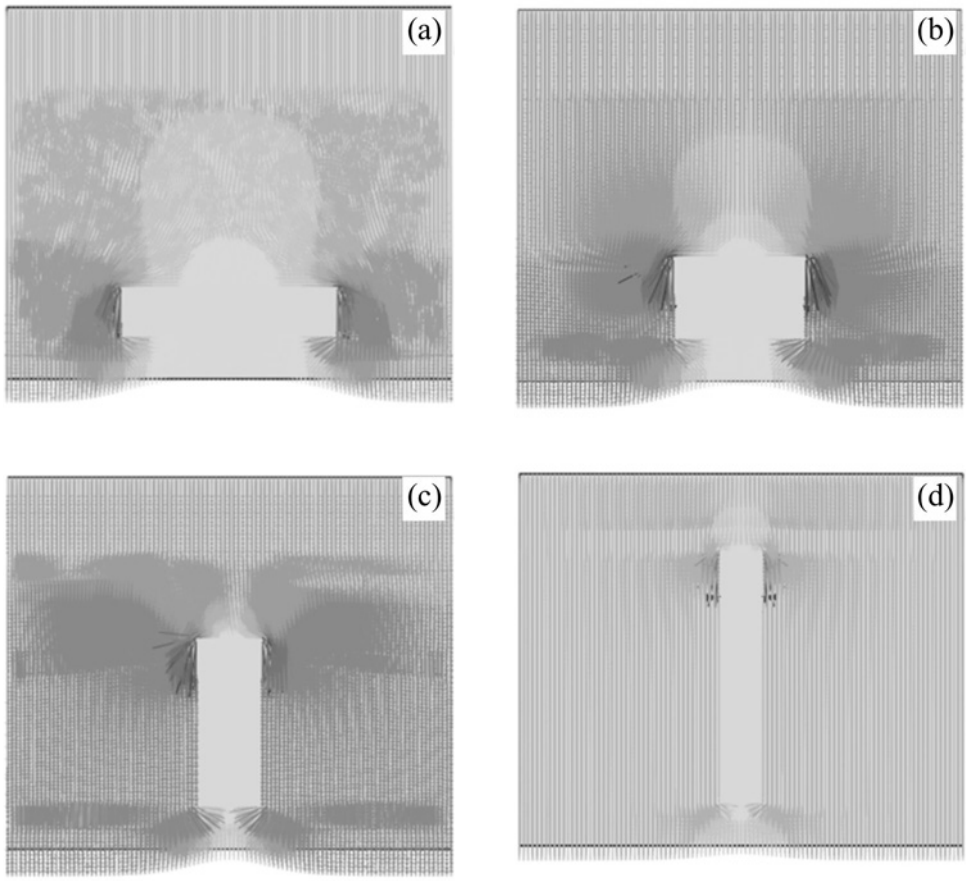

Fig. 11. Heat flux density field of the interfacial layer with pores with different aspect ratios: (a) 0.25, (b) 0.66, (c) 2.67, and (d) 6.

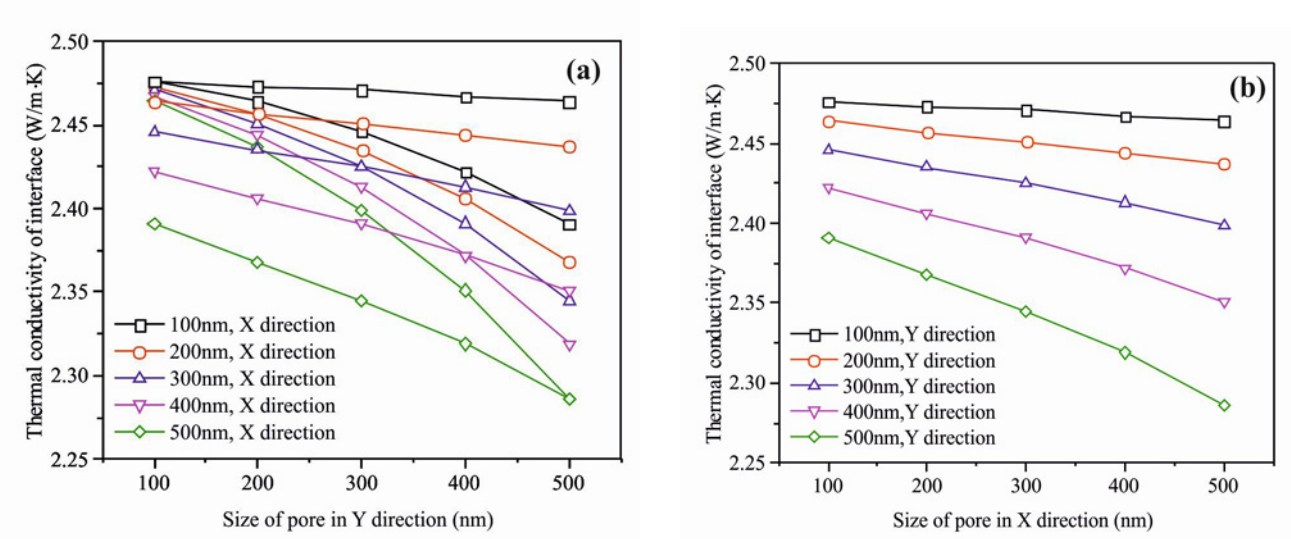

Fig. 12. Effect of the size of the pores in the (a) Y-direction and (b) X-direction on the TC of the interfacial layer.

is significantly reduced. Therefore, when the interfacial layer is discontinuous, the TC of the interfacial layer will be significantly reduced.

As shown in Fig. 11, a darker color indicates a higher heat flux density. It can be seen that the heat flux density inside the pores is extremely low because

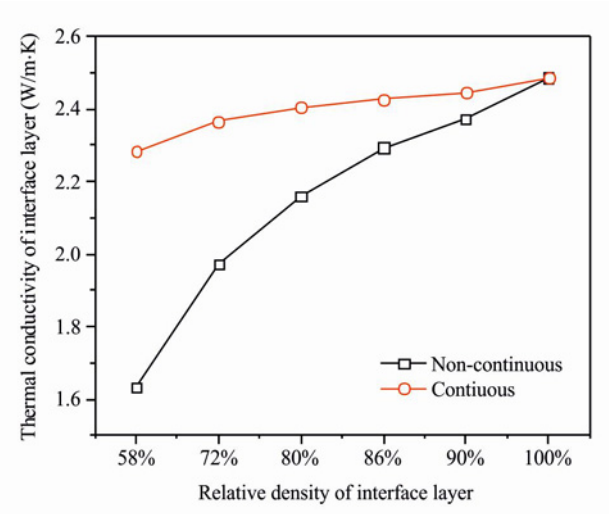

Fig. 13. TC of the interfacial layer varies with the relative density of the interfacial layer.

the TC of the pores is very low. When the heat flow encounters the pores, the heat flows around the pores. When the pore area is the same, as the aspect ratio is larger, the heat flow transfer path is shortened, the hindrance of heat flow is weakened, and $K_{\mathrm{in,p}}$ shows an upward trend.

The falling slope of the curve in Figs. 12a,b illustrates the degree of influence of the pore size in different directions on $K_{\mathrm{in,p}}$. The calculated results can provide a quantitative reference for studying the TC of pores to the interfacial layer in the experiment.

3.4.2. Effect of the relative density on the TC of the interfacial layer

It can be seen from the curve in Fig. 10 that whether the interface component is continuous or not will have an important effect on the TC of the interfacial layer. Therefore, $K_{\mathrm{in,p}}$ and K_{c} should be analyzed in two cases: the component is continuous ($K_{\mathrm{in,con}}$, $K_{\mathrm{c,con}}$) or discontinuous ($K_{\mathrm{in,dis}}$, $K_{\mathrm{c,dis}}$). Assuming that the interval of each pore distribution is 1000 nm when the component is continuous, the pore aspect ratio is 1. According to published experimental studies [19], the relative density of GFs/Cu composite (ρ_{c}) can reach more than 99.7 %. Assuming that the pores in the composite all exist at the interfacial layer, when $\rho_{\mathrm{c}} = 99.7\,\%$, the relative density of the interfacial layer is $\rho_{\mathrm{in}} = 58\,\%$. $K_{\mathrm{in,p}}$ changes with ρ_{in}, as shown in Fig. 13.

As shown in Fig. 13, both curves show an upward trend. This is because the heat transfer efficiency of the air component is low, and the pores hinder the heat flow, which makes the heat flow transfer path longer and more complicated. Therefore, as the density increases, the fewer the pores, the higher the TC of the composite. Obviously, $K_{\mathrm{in,con}} > K_{\mathrm{in,dis}}$. And as

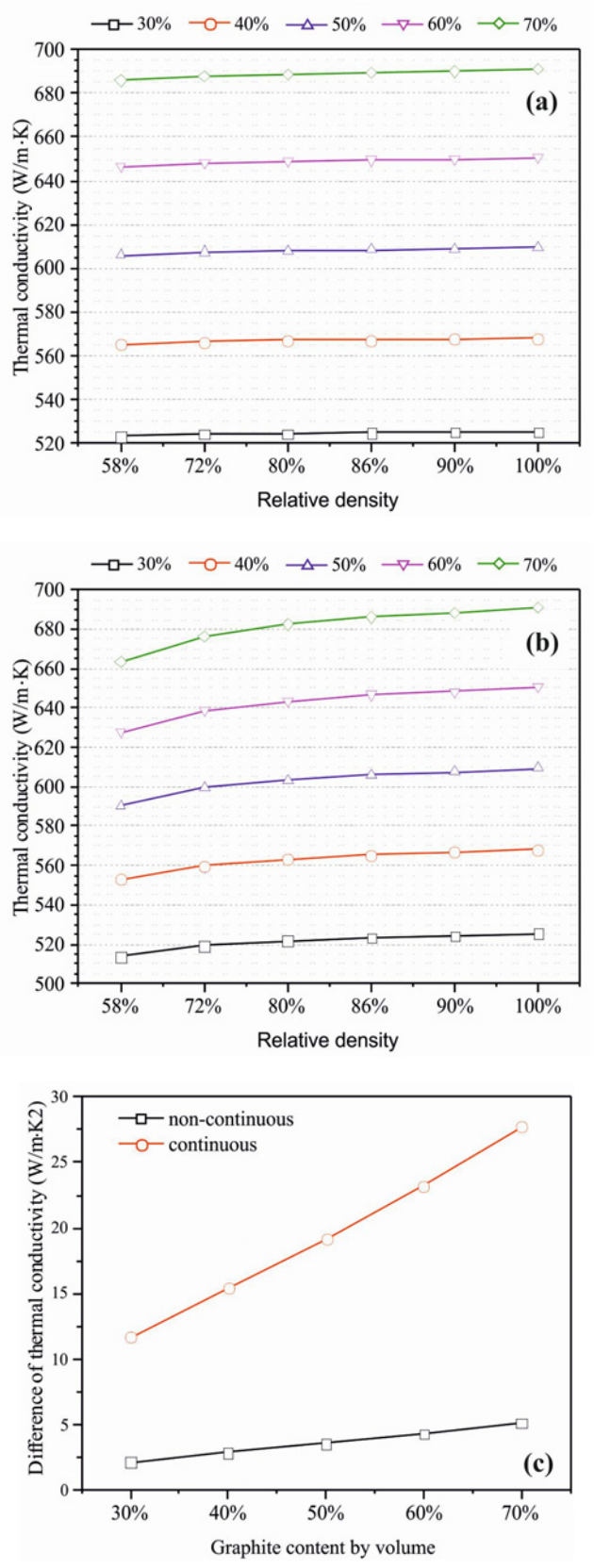

Fig. 14. Effect of interface density between (a) continuous interface and (b) discontinuous interface on the TC of composites, and (c) curve change values in (a) and (b).

ρ_{in} increases from 58 to 100 %, that is, as the pore volume fraction decreases, $K_{in,con}$ increases from 2.283 to 2.487 W m^{-1} K^{-1}, increased by 8.93 %, and $K_{in,dis}$ increases from 1.633 to 2.487 W m^{-1} K^{-1}, increased by 91 %. Corresponding to Fig. 10, this difference further illustrates that the TC of the discontinuous interface is less than the TC of the continuous one. When the thickness of the interfacial layer does not change, this change will directly reflect the change in the TC of the composite. Therefore, in the experimental preparation of particle-reinforced composites with an interfacial layer, the interface composition should be kept as continuous as possible to reduce the influence of pores on the TC of the composite.

As shown in Fig. 14, the curves show an upward trend. The more significant the volume fraction, the more pronounced the curve change trend because more interfaces are introduced, and the effect is more evident when the interface characteristics change. Compared with the continuous interface, the discontinuous change trend is more pronounced. In Fig. 14, to better compare the continuous and discontinuous cases, compare the data in Figs. 14a,b and Fig. 14c, for composite with a graphite volume fraction of 30–70 %. As V_{GF} increases, $K_{c,p}$ drop caused by pores will decrease more severely when the component of the interfacial layer is discontinuous.

4. Conclusions

In this work, the effective thermal conductivities of GFs/Cu composites with interface were calculated using FEM, following conclusions can be drawn:

As the volume fraction of GFs increases, the TC of the composite increases. As the size of GFs increases, the TC of the composite increases. When the thermal resistance of the interfacial layer is smaller, the role of the above two factors is more obvious.

The shape of the pores in the interfacial layer influences the TC of the composite. The lower the density of the interfacial layer, the lower the TC of the interfacial layer, which has a more significant impact on the composite with a high volume fraction of graphite. The TC of the composite decreases more severely when the composition of the interfacial layer is discontinuous.

The simulation calculation results in this paper can provide theoretical guidance for material manufacturing for interface design and can also be applied to other matrix composites.

Acknowledgement

This research was financially supported by “the National Natural Science Foundation of China (Grant No.51274040)”.

References

[1] X. Qu, L. Zhang, M. Wu, S. Ren, Review of metal matrix composites with high thermal conductivity for thermal management applications, Prog. Nat. Sci.-Mater. 21 (2011) 189–197. https://doi.org/10.1016/S1002-0071(12)60029-X

[2] Q. Liu, X. He, S. Ren, T. Liu, X. Qu, Effect of titanium carbide coating on the microstructure and thermal conductivity of short graphite fiber/copper composites, J. Mater. Sci. 48 (2013) 5810–5817. https://doi.org/10.1007/s10853-013-7373-y

[3] Z. Chen, Z. Tan, G. Ji, G. Fan, D. Schryvers, Q. Ouyang, Z. Li, Effect of interface evolution on thermal conductivity of vacuum hot pressed SiC/Al composites, Adv. Eng. Mater. 17 (2015) 1076–1084. https://doi.org/10.1002/adem.201400412

[4] H. Zhang, X. Ge, H. Ye, Resistance network for predicting the thermal conductivity of composite materials, J. Funct. Mater. 36 (2005) 757–759. https://doi.org/10.3321/j.issn:1001-9731.2005.05.035

[5] D. P. H. Hasselman, L. F. Johnson, Effective thermal conductivity of composites with interfacial thermal barrier resistance, J. Compos. Mater. 21 (1987) 508–515. http://doi.org/10.1177/002199838702100602

[6] N. Bonfoh, F. Dinzart, H. Sabar, New exact multi-coated ellipsoidal inclusion model for anisotropic thermal conductivity of composite materials, Appl. Math. Model. 87 (2020) 584–605. https://doi.org/10.1016/j.apm.2020.06.005

[7] D. H. Nguyen, H. L. Quang, Q. C. He, A. T. Tran, Generalized Hill-Mendel lemma and equivalent inclusion method for determining the effective thermal conductivity of composites with imperfect interfaces, Appl. Math. Model. 90 (2021) 624–649. https://doi.org/10.1016/j.apm.2020.09.026

[8] M. Gao, B. Yang, Y. Huang, G. Wang, Effects of general imperfect interface/interphase on the in-plane conductivity of thermal composites, Int. J. Heat Mass. Tran. 172 (2021) 121213. https://doi.org/10.1016/j.ijheatmasstransfer.2021.121213

[9] P. Vignesh, R. K. Kumar, M. Ramu, Evaluation of mechanical and thermal behaviour of particle-reinforced metal matrix composite using representative volume element approach, Proceedings of 2018 International Conference on Engineering Materials, Metallurgy and Manufacturing, ICEMMM (2018), pp. 415–425. ISBN: 978-981-13-1779-8

[10] C. Vieira, S. Marques, A new three-dimensional finite-volume model for evaluation of thermal conductivity of periodic multiphase composites, Int. J. Heat Mass. Tran. 139 (2019) 412–424. https://doi.org/10.1016/j.ijheatmasstransfer.2019.05.031

[11] T. Saoudi, A. E. Moumen, T. Kanit, M. Belouchrani, N. Benseddiq, A. Imad, Numerical evaluation of the thermal properties of UD-fibers reinforced composites for different morphologies, Int. J. Appl. Mech. 12 (2020) 2050032. https://doi.org/10.1142/S1758825120500325

[12] M. Zahi, R. Sharma, A. R. Bhagat, S. Abbas, A. Kumar, P. Mahajan, Micro-structurally informed finite element analysis of carbon/carbon composites for effective thermal conductivity, Compos. Struct. 226

(2019) 111221.
https://doi.org/10.1016/j.compstruct.2019.111221
[13] D. Duschlbauer, H. J. Böhm, H. E. Pettermann, Numerical simulation of thermal conductivity of MMCs: effect of thermal interface resistance, Mater. Sci. and Tech. 19 (2013) 1107–1114.
https://doi.org/10.1179/026708303225004305
[14] W. Tian, M. W. Fu, L. Qi, X. Chao, J. Liang, Interphase model for FE prediction of the effective thermal conductivity of the composites with imperfect interfaces, Int. J. Heat Mass. Tran. 145 (2019) 118796.
https://doi.org/10.1016/j.ijheatmasstransfer.2019.118796
[15] H. A. Moghaddam, P. Mertiny, Stochastic finite element analysis framework for modelling thermal conductivity of particulate modified polymer composites, Results Phys. 11 (2018) 905–914.
https://doi.org/10.1016/j.rinp.2018.10.045
[16] R. Zhang, X. He, Z. Chen, X. Qu, Influence of Ti content on the microstructure and properties of graphite flake/Cu-Ti composites fabricated by vacuum hot pressing, Vacuum 141 (2017) 265–271.
https://doi.org/10.1016/j.vacuum.2017.04.026
[17] H. Wang, J. Shang, G. Liu, X. Qin, X. Song, Overview on description methods for the spatial distribution of the second phase in multi-phase materials, Advances in Mechanics 30 (2000) 558–570.
https://doi.org/10.6052/1000-0992-2000-4-J1998-045
[18] B. Liu, D. Zhang, X. Li, H. Zhao, X. Guo, Z. Liu, Q. Guo, Effect of graphite flakes particle sizes on the microstructure and properties of graphite flakes/copper composites, J. Alloy Compd. 766 (2018) 382–390.
https://doi.org/10.1016/j.jallcom.2018.06.129
[19] D. K. Hale, The physical properties of composite materials, J. Mater. Sci. 11 (1976) 2105–2141.
http://doi.org/10.1007/bf02403361
[20] C. W. Nan, Physics of inhomogeneous inorganic materials, Prog. Mater. Sci. 37 (1993) 1–116.
https://doi.org/10.1016/0079-6425(93)90004-5
[21] P. L. Kapitza, The study of heat transfer in helium II, Helium 4 (1971) 114–153.
https://doi.org/10.1016/B978-0-08-015816-7.50014-6
[22] R. S. Prasher, P. E. Phelan, A scattering-mediated acoustic mismatch mode for the prediction of thermal boundary resistance, J. Heat Trans. 123 (2001) 105–112. https://doi.org/10.1115/1.1338138
[23] L. Silva, M. Kaviany, Micro-thermoelectric cooler: Interfacial effects on thermal and electrical transport, Int. J. Heat Mass. Tran. 47 (2004) 2417–2435.
https://doi.org/10.1016/j.ijheatmasstransfer.2003.11.024
[24] Y. Wu, J. Luo, Y. Wang, G. Wang, H. Wang, Z. Yang, G. Ding, Critical effect and enhanced thermal conductivity of Cu-diamond composites reinforced with various diamond prepared by composite electroplating, Ceram. Int. 45 (2019) 13225–13234.
https://doi.org/10.1016/j.ceramint.2019.04.008
[25] R. Prasher, Thermal boundary resistance and thermal conductivity of multiwalled carbon nanotubes, Phys. Rev. B 77 (2008) 439–446.
https://doi.org/10.1103/PhysRevB.77.075424
[26] M. Yuan, Z. Tan, G. Fan, D. Xiong, Q. Guo, C. Guo, Z. Li, Theoretical modelling for interface design and thermal conductivity prediction in diamond/Cu composites, Diam. Relat. Mater. 81 (2018) 38–44.
https://doi.org/10.1016/j.diamond.2017.11.010
[27] C. Guo, F. Sun, J. Duan, Z. Che, X. Wang, J. Wang, M. Kim, H. Zhang, Effect of Ti interlayer on interfacial thermal conductance between Cu and diamond, Acta Mater. 160 (2018) 235–246.
https://doi.org/10.1016/j.actamat.2018.09.004
[28] R. Zhang, Research on fabrication and properties of graphite flakes/Cu composites, University of Science and Technology Beijing, Beijing 2020.
https://doi.org/10.26945/d.cnki.gbjku.2020.000110
[29] X. Han, Y. Huang, X. Peng, X. Gao, T. Li, P. Liu, 3D continuous copper networks coated with graphene in Al-matrix composites for efficient thermal management, Composite Structures 258 (2021) 113177.
https://doi.org/10.1016/j.compstruct.2020.113177
[30] S. Hu, L. Lian, L. Li, Study on the thermodynamic flows and forces for complex heat-transfer process in closed space, Journal of Harbin University of C. E. & Architecture 32 (1999) 68–71.
http://en.cnki.com.cn/Article_en/CJFDTOTAL-HEBJ199903014.htm
[31] Air – Thermophysical Properties, Engineering Tool-Box, (2003). https://www.engineeringtoolbox.com/air-properties-d_156.html